Biosensors and Bioelectronics 147 (2020) 111737

Contents lists available at ScienceDirect

Biosensors and Bioelectronics

journal homepage: http://www.elsevier.com/locate/bios

Interfacial charge regulation of protein blocking layers in transistor biosensor for direct measurement in serum

Sungwook Park [a,b], Minsoo Kim [a,c], Dongkap Kim [a,c], Seok Ho Kang [d], Kwan Hyi Lee [a,b,**], Youngdo Jeong [a,b,*]

[a] Center for Biomaterials, Biomedical Research Institute, Korea Institute of Science and Technology (KIST), 5 Hwarangno 14-gil, Seongbuk-gu, Seoul, 02792, Republic of Korea
[b] Division of Bio-Medical Science & Technology, KIST School - Korea University of Science and Technology (UST), 5 Hwarangno 14-gil, Seongbuk-gu, Seoul, 02792, Republic of Korea
[c] Department of Chemistry, Hanyang University, 222, Wangsimni-ro, Seongdong-gu, Seoul, 04763, Republic of Korea
[d] Department of Urology, Korea University School of Medicine, 73, Inchon-ro, Seongbuk-gu, Seoul, 02841, Republic of Korea

ARTICLE INFO

Keywords:
Protein blocking layer
Field-effect transistor
Serum
Non-specific binding
Biosensor

ABSTRACT

Ion-sensitive field-effect transistor (ISFET) as a biosensor facilitates a process of data-acquisition through label-free and real-time monitoring. Direct quantification of a biomarker in serum is challenging in ISFET biosensor since charged proteins in serum interfere transduction to electrical signals. Here, we report the fabrication of protein blocking layers (PBLs) with intended interfacial charges to minimize non-specific protein bindings on ISFET. Use of charged protein precursors enables to regulate the interfacial charge of PBLs, preserving their intrinsic electric features (neutral: hemoglobin, positively charged: lysozyme, negatively charged: BSA). The effect of this interfacial charge on the signal was demonstrated through PSMA (prostate cancer biomarker) sensing using a dual-gate ISFET biosensor. The neutral PBL showed the minimum noise compared to the negatively and positively charged PBLs, enabling the ISFET to exhibit the same detection range in untreated serum as with pre- or post-treatment (1 fg/ml to 100 ng/ml). The introduction of neutral PBLs to ISFET biosensors would allow the application of the ISFET biosensor as a point-of-care device.

1. Introduction

Precise transduction of a specific biological event into electric signals using ion-sensitive field-effect transistors (ISFETs) is a potential means of diagnosing infections, diseases, and cancers by an electronic device (Choi et al., 2017b; Hwang et al., 2017; Kaisti, 2017; Maehashi et al., 2007; Nakatsuka et al., 2018). However, it is challenging to directly detect a biomarker in serum that contains 20,000 proteins since undesirable protein bindings interfere with electrical signals (De et al., 2009). Nonspecifically absorbed proteins on the sensing membrane of ISFETs not only induce noise but also shorten the Debye screening length (<1 nm) by increasing a local accumulation of ions due to their intrinsic charge (Chu et al., 2017; Syu et al., 2018). Pre-treatment, such as filtration, desalting, and dilution of a serum, or post-treatment including washing, can address this problem, but these procedures complicate the measurement protocol, increasing the possibility of diagnostic errors. Additionally, the post-treatment process diminishes benefits of real-time detection in ISFET sensors (Choi et al., 2017a).

Introduction of blocking layers on ISFET biosensors can be an approach to inhibit non-specific protein bindings on the sensing membrane. For the fabrication of blocking layers, various methods that use synthetic materials (ethanolamine, polyethylene glycol, and surfactants) (Aliakbarinodehi et al., 2017; Hao et al., 2017; Hsiao et al., 2009; Huang et al., 2015; Regonda et al., 2013; Villamizar et al., 2008), natural materials (BSA or casein) (Basu et al., 2018; Gong et al., 2019; Hideshima et al., 2012; Presnova et al., 2017), or their combinations (Andoy et al., 2018; Cheng et al., 2014; Gao et al., 2016; Gutierrez-Sanz et al., 2017; Rajesh et al., 2016) have been attempted. Among these materials, BSA

* Corresponding author. Center for Biomaterials, Biomedical Research Institute, Korea Institute of Science and Technology (KIST), 5 Hwarangno 14-gil, Seongbuk-gu, Seoul, 02792, Republic of Korea.
** Corresponding author. Center for Biomaterials, Biomedical Research Institute, Korea Institute of Science and Technology (KIST), 5 Hwarangno 14-gil, Seongbuk-gu, Seoul, 02792, Republic of Korea.
E-mail addresses: kwanhyi@kist.re.kr (K.H. Lee), zerodegree@kist.re.kr (Y. Jeong).

https://doi.org/10.1016/j.bios.2019.111737
Received 5 August 2019; Received in revised form 19 September 2019; Accepted 27 September 2019
Available online 10 October 2019

has been widely employed as a blocking agent due to their enzymatic inactivity, abundance in biology, biocompatibility, and stability in many biochemical reactions. The BSA layers reduce the surface energy between the sensing membrane and serum that is the main cause of non-specific protein binding (Latour et al., 2008). However, the charge effect of the blocking layer on sensing signals has not been considered yet. The charge of as-prepared blocking layers could induce undesirable electrostatic binding between the blocking layer and the serum proteins, interfering with the signal (Aramesh et al., 2015; Ruggeri et al., 2013; Soler et al., 2014). As-induced noise can be negligible in low sensitive ISFET biosensors, but it causes false positives or true negatives in the case of ultralow concentration detection using highly sensitive ISFET biosensors such as dual-gate transistor-based biosensors (Choi et al., 2019; Jeun et al., 2017, 2019; Seong et al., 2018). To overcome this issue, a systematic study about the charge effects of the blocking layer on the signal of highly sensitive ISFET biosensor is required.

Here, we report the fabrication of protein blocking layers (PBLs) with neutral, negatively charged, or positively charged properties to investigate the effect of surface charge of the blocking layer on the signal of a highly sensitive ISFET biosensor (Scheme 1). A dual-gate ISFET biosensor was used to detect minute signal changes as a result of the blocking layers' charge. As a target protein and receptor, we chose the PSMA (prostate cancer biomarker) and its antibody, respectively. The PBL consisting of neutral proteins (hemoglobin, Hemo) showed a more inhibitory feature of the non-specific binding attributed serum proteins than negatively charged (BSA) or positively charged (lysozyme, Lyso) PBL, suppressing the generation of noise. As a result, the biosensor with the neutral PBLs could detect the PSMA protein in fg/ml range in serum without post-treatment while the biosensor with negatively or positively charged PBLs could not. The detection range at the biosensor with negative or positive PBL was from 0.1 pg/ml to 1 ng/ml in untreated serum, but the biosensor with neutral blocking layer has the detection range of 1 fg/ml-100 ng/ml. Based on this investigation of blocking layers' charge effect on the signal, the design of blocking layers would allow for the direct detection in untreated serum without post-treatment, enhancing the sensing performance.

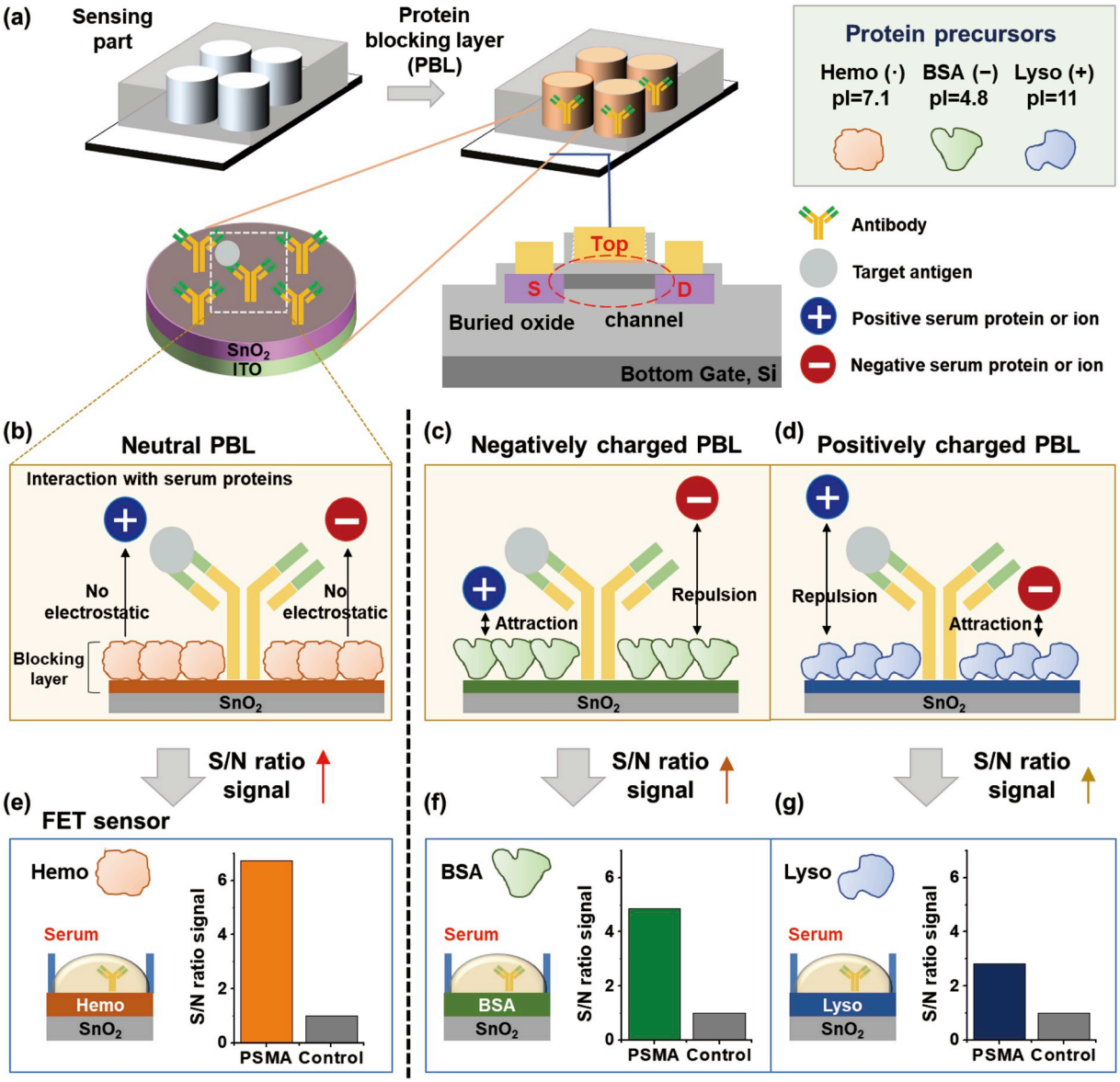

Scheme 1. Schematic illustration of the PBLs' charge effect on the ISFET biosensor. (a) Structure of dual-gate ISFET biosensor with sensing part with protein blocking layers. Interaction with serum proteins and PBLs consisting of (b) Hemo, (c) BSA, and (d) Lyso. Signal-to-noise ratio in the condition of 1 ng/ml PSMAs at with/without antibody by the ISFET biosensor applied PBLs ((e) Hemo PBL, (f) BSA PBL, (g) Lyso PBL).

2. Experimental section

2.1. Materials and reagents

For the fabrication of the PBLs, human serum (H4522), human hemoglobin (H7379), human lysozyme (L1667), 3-aminopropyltriethoxysilane (APTES), and glutaraldehyde were purchased from Sigma Aldrich. Bovine serum albumin (BSA, 97061-416) was purchased from VWR. For the ISFET biosensor, Human PSMA protein (orb245517), and anti-PSMA antibody (orb25921) were bought from Biorbyt. For gold nanoparticle synthesis, gold(III) chloride trihydrate ($HAuCl_4 \cdot 3H_2O$), azobisisobutyronitrile (AIBN), thioacetic acid, trimethyl amine (NMe_3), mercaptoundecanoic acid (MUA), and sodium methoxide (NaOMe) were purchased from Sigma Aldrich. Sodium borohydride ($NaBH_4$) was purchased from Acros Organics. 10-undecenyl bromide was purchased from TCI, Japan. For the characterization of the PBLs, highly-oriented pyrolytic graphite (HOPG) was obtained from Bruker. Quartz glass (RE.10101, 10 mm × 10 mm) was purchase from iNexus.

2.2. Fabrication of dual-gate ISFET biosensor

The dual-gate ISFET biosensor was consist of two parts including a FET device and a sensing part. The FET was fabricated following methods described in the literature (Choi et al., 2019; Jeun et al., 2017, 2019; Park et al., 2017). In brief, a 6-inch p-type (100) silicon wafer consisting of a 750 nm buried oxide layer and a 100 nm top silicon layer was used. Photolithography and inductively coupled plasma reactive-ion etching (ICP-RIE) were employed to define the active region. A 10 nm thick top gate oxide layer was deposited by a dry oxidation process. A Ti/TiN/Al/TiN multilayer was grown on the layer via a sputtering system, and it was then etched by ICP-RIE to form the gate electrode. The arsenic (As) ion implantation formed source and drain regions.

A film on the indium tin oxide (ITO, 300 nm) on glass substrate was prepared for the fabrication of the sensing part. For the PDMS wells, Sylgard 184's base and curing agent were formulated with a ratio of 10:1. As-mixture was cured at 60 °C for 3 h. These PDMS wells were attached to ITO after O_2 plasma treatment (70 W, 30 sccm of O_2 gas flow for 1 min, Plasma System Cute, Femto Science). An annealing process was carried out at 60 °C for 10 min.

2.3. Surface modification for PBLs on the sensing membrane

The OH groups were formed on the surface of the sensing part by O_2 plasma treatment at 70 W for 1 min. Then NH_2 groups were introduced by dipping the surface in 5% APTES in ethanol for 1 h. After washing, we cured the APTES layers at 120 °C for 30 min. To make an amide bond with antibodies or proteins, 2.5% glutaraldehyde solution was used to treat the APTES layer. The surface was then chemically modified by adding antibodies through incubation in 5 μg/mL of antibodies for 1 h at room temperature. To fabricate the PBLs on the sensing membrane, we incubated the surface in 1% Hemo, BSA, and Lyso solution for 1 h.

2.4. Surface charge characterization of PBLs

KPFM: ITO glasses deposited with SnO_2 and PBLs were prepared as 1 cm × 1 cm. The surface potential of PBLs were analyzed with KPFM mode using AFM (XE-100, Park Systems). The scan rate and amplitude were 0.25 Hz and 2 V, respectively. During the measurement, we used a gold-coated silicon cantilever (NSC14/Cr-Au, a force constant of 5 N/m, and a resonance frequency of 160 kHz). The measurements were performed in a closed chamber for noise reduction under ambient temperature and atmospheric conditions.

Surface zeta potential (SZP): 3 mm × 3 mm ITO glasses deposited with SnO_2 and PBLs on SnO_2 were prepared. The samples were attached to a zeta potential cell using double-sided Scotch tape, and then as-prepared cells were loaded into the instruments (Zetasizer ZSP, Malvern). The measurement duration was automatically adjusted. As a tracer, zeta potential transfer standard (−42 ± 4.2 mV, DTS1235, Malvern) was used. The zeta potential values were obtained according to the distance between tracers and the surface (125, 250, 375, and 500 μm). Then the surface zeta value was calculated by extrapolating to zero displacement and a tracer zeta potential value of 1000 μm above the surface (Fig. S1).

Charged particle adhesion: 2 nm-gold nanoparticles with negatively or positively charged surface ligands were synthesized by multistep Brust–Schiffrin synthesis coupled with the Murray-place exchange reaction (Hostetler et al., 1999). As positively and negatively charged ligands, N, N, N-trimethyl-11-sulfanyl-1-undecanaminium chloride (TMA), and mercaptoundecanoic acid (MUA) were used, respectively. The synthesized positively or negatively charged gold nanoparticles were treated on each PBL for 20 min. After washing, we measured the I_D-V_G curve using the ISFET biosensor or carried out the silver staining of the PBLs to monitor the electrostatic adhesion of charged gold nanoparticles. After silver staining for 30 min, we observed the surface using optical microscopy (Leica DM IL LED).

2.5. Detection of PSMA in serum with the ISFET biosensor

We used a dual-channel parameter analyzer (4200A-SCS, Keithley) to obtain an I_D-V_G curve using on ISFET. For the I_D-V_G curve, the sweeping voltage of bottom gate and drain voltage were −5 to +5 V and 3 V, respectively. To obtain the standard curve, we plotted the voltage change according to the concentration of PSMA (1 fg/mL to 100 ng/mL). The initial voltage value was determined as the V_G value at 10 nA in I_D-V_G curves. After a 20 min incubation in the PSMA solution, the detection voltage was measured at 10 nA. The incubation time was optimized (Fig. S2). There was no washing process for the direct quantification in serum. For the pre- and post-conditioning process, the V_G value was measured after washing with a 1 × PBS. FET responses depending on the concentration of PSMA were fit to the Hill equation, which is formally equivalent to the Langmuir isotherm: $Y = V_{max}*(X^n)/(K_d^n + X^n)$, where V_{max} is the maximum specific binding extrapolated to high concentrations of the target (saturation), X is the target concentration, K_d is the target concentration necessary to achieve half-maximum binding at equilibrium, and n is the Hill slope, which was allowed to vary.

3. Results and discussion

3.1. Fabrication of PBLs

For probing the charge effect of PBLs on the sensing performance of ISFET biosensor, we fabricated three PBLs with different charges on sensing part of the ISFET biosensor system. For the neutral, negatively charged, and positively charged PBLs, hemoglobin (Hemo, pI = 7.1), BSA (pI = 4.8), and lysozyme (Lyso, pI = 11) were employed as protein precursors due to their intrinsic charge at pH 7.4. After the formation of PBLs, the surface charge of the Hemo PBL, BSA PBL, Lyso PBL, and HOPG as a control were examined using KPFM and SZP to confirm the retention of the protein precursors' electrostatic features at the macroscopic layer. The KPFM measured the local work function difference between a metalized probe (Au) and the protein surfaces (Sinensky and Belcher, 2007). The histograms of the measured surface potential contrast relative to the neutral HOPG substrate. This indicates that Hemo, BSA, and Lyso PBLs could preserve their original electrostatic features of neutral, negative, and positive surface potentials, respectively (Fig. 1a and Fig. S3). From SZP in terms of the distance between the PBLs and the charged tracer beads, we calculated the SZP of Hemo, BSA, and Lyso PBLs. Hemo PBL showed relatively neutral SZP (2.94 mV) while the BSA PBL and the Lyso PBL possessed negative and positive zeta potential, showing −29.8 mV and +8.5 mV, respectively (Fig. 1b and Fig. S1). The charge of PBLs was further examined through

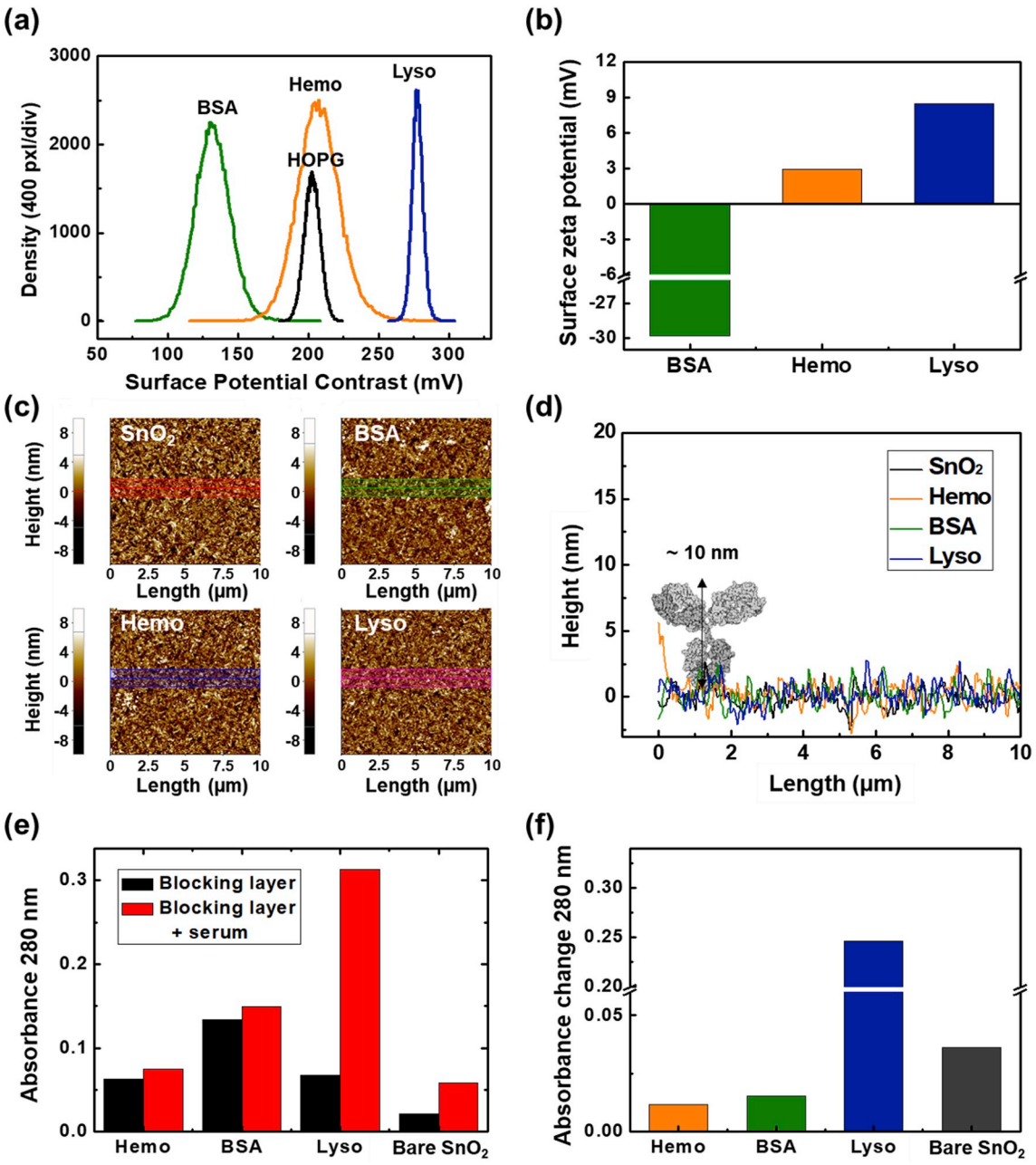

Fig. 1. The surface potential of SnO_2 and the PBLs by (a) KPFM and (b) SZP. (c) AFM images of bare sensing surface and PBLs. (d) Height analysis of PBLs. (e) UV-vis absorbance of quartz glass with the PBL before/after incubation in untreated serum and mild wash. (f) Absorbance change of PBLs by non-specific binding from serum proteins.

charge-selective adhesion of positively and negatively charged gold nanoparticles (Fig. S4). The results corresponded with the surface charge differences observed by KPFM and ZSP, showing that the surface of the PBLs preserved the proteins' original surface charge.

We next, investigated the surface roughness of all PBLs using AFM to confirm whether the PBLs hinder the binding between a target antigen and an antibody. Based on the AFM images of the PBLs, the surface roughness of bare SnO_2, BSA, Hemo, and Lyso PBL were 2.534, 3.174, 3.262, and 3.252 nm at the area of 10 μm × 10 μm, indicating that the PBLs were well formed without aggregations regardless of the type of PBL (Fig. 1c). From the cross-sectional height profile of all PBLs, we can assume that the PBLs are unable to hinder antigen-antibody recognition considering the size of the antibody (~10 nm) (Fig. 1d).

To probe non-specific protein binding on each PBL in the untreated serum, the amount of adsorbed proteins on the PBL was obtained by surface UV-vis spectrometry after the treatment of the serum (Fig. 1e and f). We first, fabricated each PBL on quartz glass and measured the UV absorbance of the substrate before and after the serum incubation for 1 h to induce non-specific binding. While UV absorbance of the Lyso PBL increased after serum incubation, the absorbance of Hemo PBL and BSA PBL showed the negligible change, indicating much more non-specific binding occurred with Lyso PBL than others. Since the untreated serum contains a large portion of negative proteins, for example~ 60% human serum albumin (pI = 4.7), we assumed that the positive surface potential of the Lyso PBL induced more non-specific bindings via electrostatic interactions. The non-specific binding in the untreated serum could be diminished through the regulation of the surface charge potential of the PBLs.

3.2. Electrical characteristics of ISFET according to PBLs

To evaluate the charge effect of the PBLs on the signal of the ISFET biosensor, we investigated indicators of electrical performance such as transfer curves (I_D-V_G), output characteristic curves (I_D-V_D), and pH sensitivity. We first, prepared the PBLs on the sensing part of the ISFET biosensor and then measured the electrical properties in 1 × PBS. I_D-V_G and I_D-V_D curves were measured by a bottom gate sweep under a dual-gate operation (Fig. 2a and b). On/off current ratios and the sub-threshold wing were $>10^6$ and 1871 mV/dec respectively, regardless of the Hemo, BSA, and Lyso PBLs. The pH sensitivity of the ISFET biosensor with the PBLs was determined by measuring the I_D-V_G curves in pH 4, pH 7, and pH 10, showing similar pH sensitivity on all PBLs (Fig. 2c–e). These results indicate that the formed PBLs are unable to affect the ISFET electrical performance, for the inference that the signal difference between the PBLs was only caused by the non-specific bindings on the PBLs in the same measurement conditions.

3.3. Signal stability according to PBLs in measurement condition

During a sensing process, electrolytes usually generate voltage drift error in ISFET biosensors, affecting a detection signal (Aliakbarinodehi et al., 2017). A blocking layer can alleviate the voltage drift error in an ISFET biosensor. To examine the reducing effect of drift error in each PBL, we measured the voltage change (ΔV_{BG}) in untreated serum incubated for 20 min, considering the direct measurement in serum (Fig. 3a). Among PBLs, the voltage change of the Hemo PBL showed the lowest (170 ± 11 mV), while the Lyso PBL showed the highest (270 ± 25 mV). In 1 × PBS (Fig. 3b) and in serum that underwent washing (Fig. 3c), the signal drift of each PBL also was evaluated considering the pre-conditioning, such as buffer change or dilution, and the post-conditioning. In these two conditions, the neutral Hemo PBL showed the lowest voltage change, demonstrating the PBLs' neutral feature effectively inhibits the drift error. In contrast, the negative BSA PBL and positive Lyso PBL attracted oppositely charged ions and proteins which increased the drift.

We hypothesized that the charged PBLs attract the materials with counter-charge, and were then recognized as a signal in ISFET biosensor. As a model system for the demonstration, we used positively (TMA) and negatively (MUA) charged gold nanoparticles to mimic the charged bio-entities (Cho et al., 2017; Saha et al., 2012). When the MUA and TMA nanoparticles were treated in the biosensor, the biosensors with Lyso PBL and the BSA PBL showed the highest drift error, respectively as expected (Fig. 3d and e). Meanwhile, in both environments, the Hemo PBL exhibited the lowest drift error, supporting our hypothesis (Fig. 3f).

3.4. Signal sensitivity according to PBLs in various measurement condition

To confirm the enhancement of the sensing performance upon regulating the surface charge of PBLs, we measured the voltage change from I_D-V_G curve as a signal in terms of PSMA concentration (1 fg/ml-100 ng/ml). In the direct measurement in untreated serum, the biosensor with Hemo PBL could detect PSMA at 1 fg/ml, while the detection limit of the biosensor with BSA and Lyso PBLs was 100 fg/ml. This indicates that non-specific binding induced by the surface charge of PBLs interfered the signals. The ISFET biosensor with Hemo PBL was more sensitive at all concentrations compared to the BSA and Lyso PBLs except the BSA PBL at 1 ng/ml (Fig. 4a and b). Considering the pre-conditioning, we observed the detection signals in the condition of 1 × PBS incubation. The detection signals of the biosensor with Hemo PBL were the highest in the detection range of 100 fg/ml to 100 ng/ml. In these conditions, the ISFET biosensor with BSA PBL could detect the PSMAs in 1 fg/ml (Fig. 4c). Additionally, in the 1 × PBS, we calculated the ΔV_{max} and K_d using the Hill-Langmuir equation to investigate the PBLs' charge effect on Debye length. While the biosensor with Hemo PBLs possessed 2.07 ± 0.12 V (V_{max}), the BSA and Lyso PBLs had 1.71 ± 0.17 V, and 0.78 ± 0.21 V, respectively, indicating that the charge of the PBLs increased the local concentration of ions, which shortens the Debye length (Sun and Liu, 2018). The K_d value between

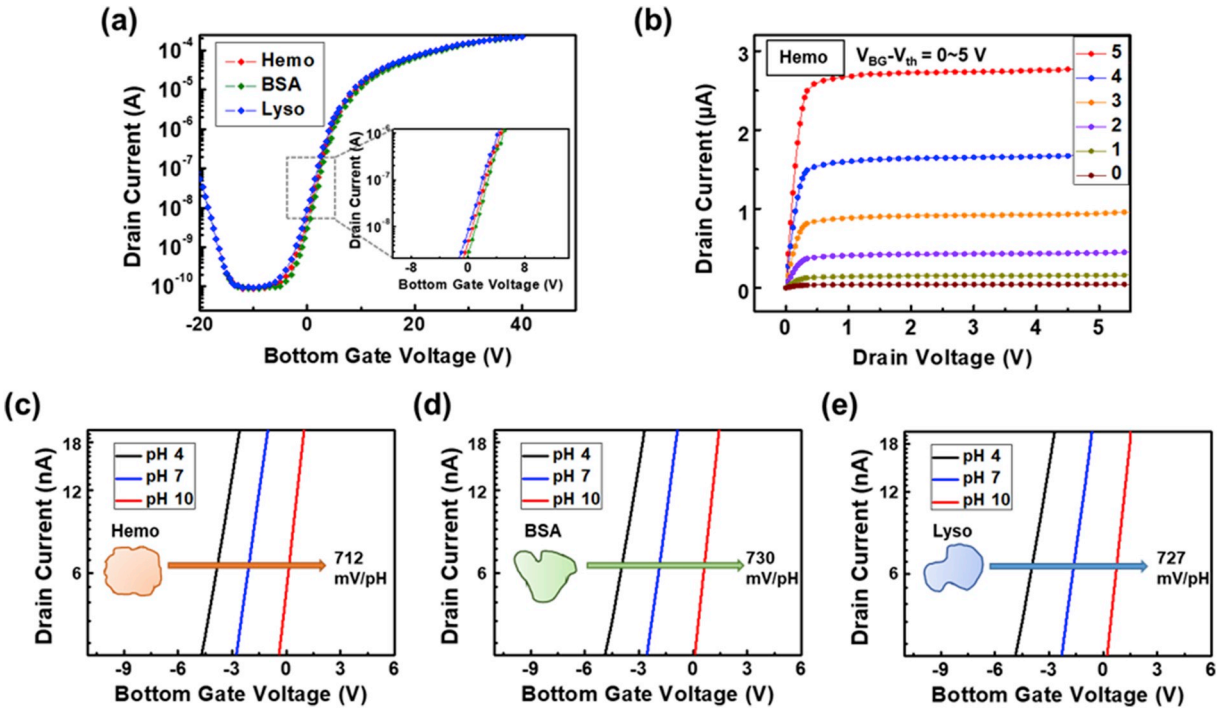

Fig. 2. (a) Transfer curves of ISFET biosensor with PBLs measured under bottom gate sweep. (b) Output characteristic curves of ISFET biosensor with Hemo PBL. (Sweep drain voltage: 0 V–5 V) The pH sensitivity of the ISFET biosensor with PBLs ((c) Hemo, (d) BSA, and (e) Lyso) in buffer solutions with pH 4, 7, and 10. The variation of V_{BG} according to pH were measured at 10 nA, sweep gate voltage: − 20 V ~ + 40 V.

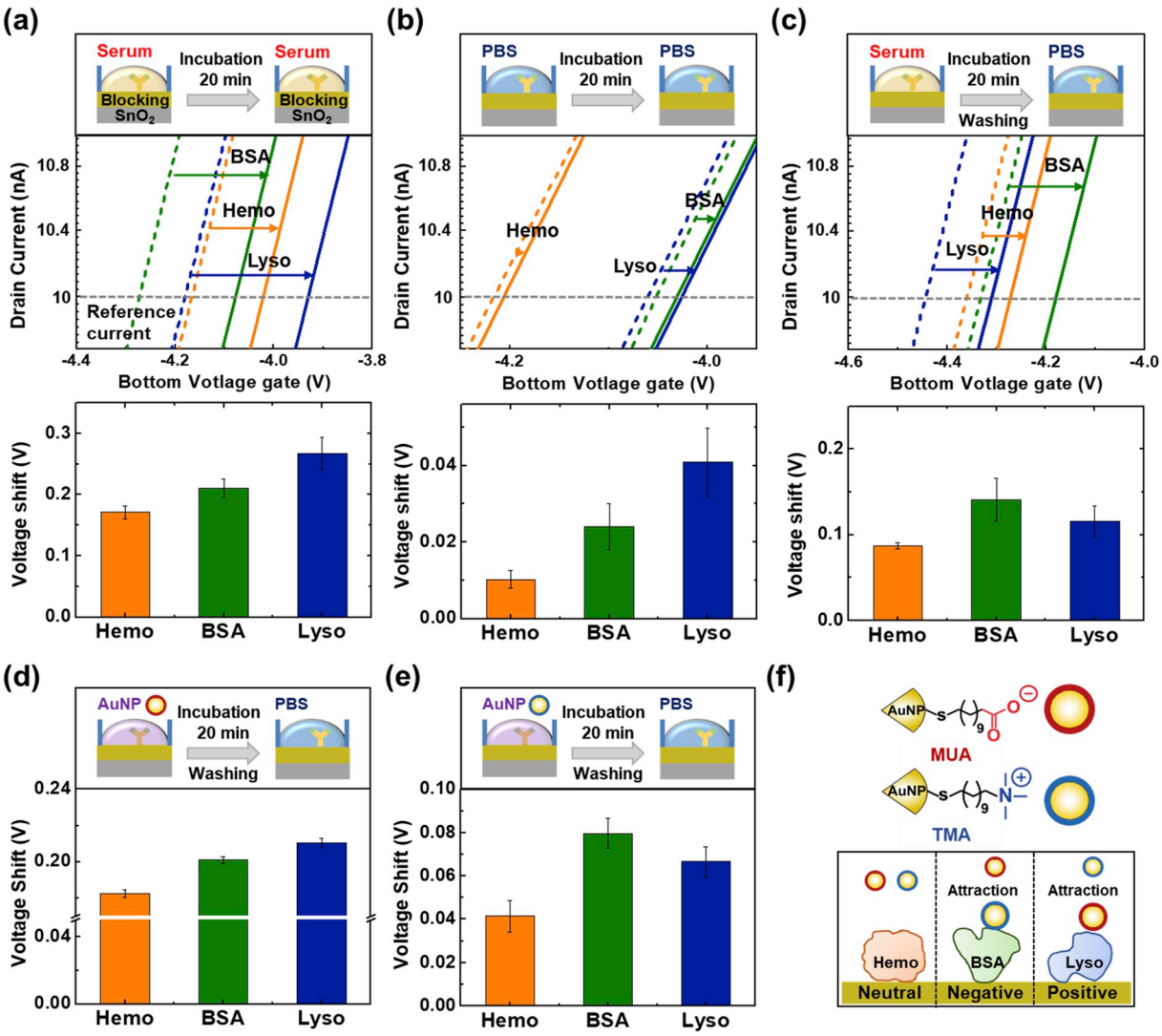

Fig. 3. Non-specific signals of the ISFET biosensor with the PBLs. I_D-V_{BG} curves and variation of V_{BG} (a) in untreated serum without pre and post-conditioning. The initial curve and final curve were presented by the dotted line and the solid line, respectively. I_D-V_{BG} curves and variation of V_{BG} (b) in 1 × PBS (implying for pre-conditioning). I_D-V_{BG} curves and variation of V_{BG} (c) in untreated serum with washing and buffer exchange with 1 × PBS (implying for post-conditioning). The variation of all samples was measured after 20 min incubation. Variation of V_{BG} in 1 × PBS in the presence of (d) negatively and (e) positively charged gold nanoparticle (MUA, TMA, respectively; both 150 nM). (f) The schematic illustration for the attraction between the PBLs and charged nanoparticles. All the samples were measured in triplicate. The variation of V_{BG} was measured at 10 nA, sweep gate voltage: − 20 V ~ + 40 V.

antibody and PSMAs can be affected by ion strength (Reverberi and Reverberi, 2007). From the lowest K_d value $(1 \pm 1) \times 10^{-12}$ of the FET biosensor with neutral PBLs, we can assume that the charge of PBLs related to local ion strength on the sensing membrane. (BSA PBL K_d $(5 \pm 8) \times 10^{-12}$ g/ml; Lyso PBL K_d $(2 \pm 6) \times 10^{-9}$ g/ml) Based on this result, the use of the neutral PBLs minimized this effect, improving the performance.

The performance of the ISFET biosensor in post-conditioning, serum incubation with washing process and buffer change, showed similar detection ranges regardless of the PBLs, but detection signals were slightly higher in the ISFET sensor with Hemo PBL (Fig. 4d). This result implies that we could remove the electrostatically bound serum proteins from the PBLs through the washing process. However, in the post-conditioning, the differentiation at a high concentration range of PSMA (1–100 ng/ml) was limited, presumably resulting from the dissociation of PSMA through washing. Collectively, we could lower the detection limit of direct measurement in serum upon regulating the charge of the PBLs.

4. Conclusions

In this study, we fabricated the charged PBLs on the sensing membrane of ISFET biosensors for minimizing the noise from non-specific protein binding. The charge of PBLs was regulated by the selection of protein precursors (positively charged: lysozyme, negatively charged: BSA, neutral: hemoglobin). After the chemical adsorption of the precursors to form the PBLs on the sensing membrane, the PBLs retained their inherent charges of the precursors, which is evidenced by KPFM, SZP, and charged particle adhesion. The charge effect of each PBLs on the sensing signal was demonstrated by comparing to the PSMA (prostate cancer biomarker) detection of the ISFET biosensor in untreated serum, with/without pre- or post-conditioning. The ISFET biosensor with neutral PBL showed minimum drift error, the broader detection range, and higher signals than the charged PBLs in all of the conditions. The detection range for PSMA was from 1 fg/ml to 100 ng/ml in untreated serum, which is the same detection range with pre- or post-conditioning. This result indicates the introduction of the neutral PBLs allows the omission of the pre- or post-treatment of serum. The direct

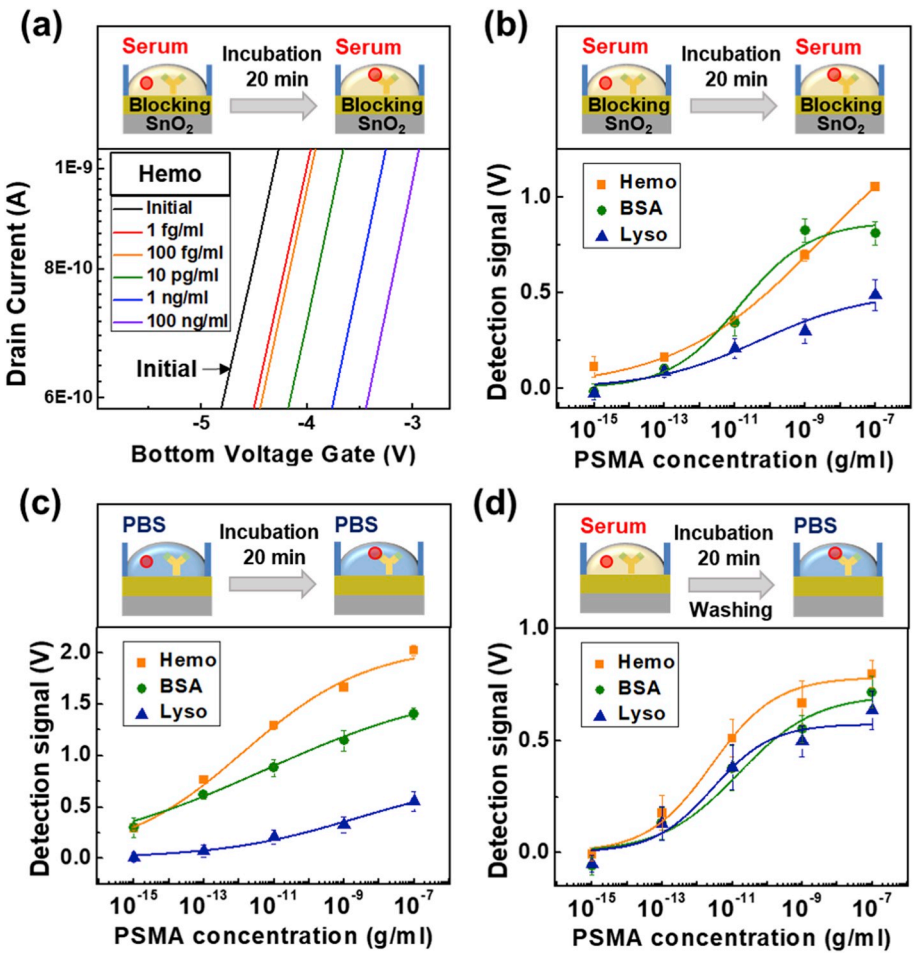

Fig. 4. Standard curves of the ISFET biosensor. (a) I_D-V_{BG} curves (Hemo PBL) in the condition of direct measurement. V_{BG} variation of the ISFET biosensor according to PSMA concentrations in the condition of (b) direct measurement in untreated serum, (c) after pre-conditioning of the sample, and (d) after post-conditioning. The detection signals were normalized by subtracting the buffer voltage drift. All the samples were tested in triplicate. The variation of V_{BG} was measured at 10 nA, sweep gate voltage: − 20 V ~ + 40 V. The results were fit to the Hill equation: $Y = V_{max} \times (\frac{X^n}{K_d^n + X^n})$

quantification of a specific biomarker in untreated serum through our method would pave a new road for the development of transistor biosensors as a point-of-care device. The neutral PBLs fabricated with hemoglobin still allow non-specific protein binding in serum. Further studies will be performed using a strategy of a blend of protein precursors or synthetic materials in order to more precise interfacial charge control.

Declaration of competing interest

The authors declare that they have no known competing financial interests or personal relationships that could have appeared to influence the work reported in this paper.

CRediT authorship contribution statement

Sungwook Park: Conceptualization, Formal analysis, Writing - original draft. **Minsoo Kim:** Formal analysis. **Dongkap Kim:** Formal analysis. **Seok Ho Kang:** Formal analysis. **Kwan Hyi Lee:** Conceptualization, Formal analysis, Writing - original draft. **Youngdo Jeong:** Conceptualization, Formal analysis, Writing - original draft.

Acknowledgements

This research was supported by the Bio & Medical Technology Development Program of the NRF funded by Republic of Korea MSIP (2015M3A9E2029265), R&D Convergence Program of National Research Council of Science & Technology (NST) of Republic of Korea (CAP-16-02-KIST) and, KIST institutional program (#2E29340) of Republic of Korea.

Appendix A. Supplementary data

Supplementary data to this article can be found online at https://doi.org/10.1016/j.bios.2019.111737.

References

Aliakbarinodehi, N., Jolly, P., Bhalla, N., Miodek, A., De Micheli, G., Estrela, P., Carrara, S., 2017. Sci. Rep. 7, 44409.
Andoy, N.M., Filipiak, M.S., Vetter, D., Gutierrez-Sanz, O., Tarasov, A., 2018. Adv. Mater. Technol. 3 (12), 1800186.
Aramesh, M., Shimoni, O., Ostrikov, K., Prawer, S., Cervenka, J., 2015. Nanoscale 7 (13), 5726–5736.
Basu, J., Baral, A., Samanta, N., Mukherjee, N., Roychaudhuri, C., 2018. J. Electrochem. Soc. 165 (8), B3201–B3207.
Cheng, S.S., Hotani, K., Hideshima, S., Kuroiwa, S., Nakanishi, T., Hashimoto, M., Mori, Y., Osaka, T., 2014. Materials 7 (4), 2490–2500.
Cho, S., Park, W., Kim, D.H., 2017. ACS Appl. Mater. Interfaces 9 (1), 101–111.
Choi, D.H., Li, Y., Cutting, G.R., Searson, P.C., 2017. Sens. Actuators B Chem. 250, 673–678.
Choi, J., Jeun, M., Yuk, S.S., Park, S., Choi, J., Lee, D., Shin, H., Kim, H., Cho, I.J., Kim, S. K., Lee, S., Song, C.S., Lee, K.H., 2019. ACS Nano 13 (1), 812–820.
Choi, J., Seong, T.W., Jeun, M., Lee, K.H., 2017. Adv. Healthc. Mater. 6 (20), 1700796.
Chu, C.H., Sarangadharan, I., Regmi, A., Chen, Y.W., Hsu, C.P., Chang, W.H., Lee, G.Y., Chyi, J.I., Chen, C.C., Shiesh, S.C., Lee, G.B., Wang, Y.L., 2017. Sci. Rep. 7, 5256.
De, M., Rana, S., Akpinar, H., Miranda, O.R., Arvizo, R.R., Bunz, U.H.F., Rotello, V.M., 2009. Nat. Chem. 1 (6), 461–465.
Gao, N., Gao, T., Yang, X., Dai, X.C., Zhou, W., Zhang, A.Q., Lieber, C.M., 2016. Proc. Natl. Acad. Sci. U.S.A. 113 (51), 14633–14638.
Gong, H., Chen, F., Huang, Z.L., Gu, Y., Zhang, Q.Z., Chen, Y.J., Zhang, Y., Zhuang, J., Cho, Y.K., Fang, R.N.H., Gao, W.W., Xu, S., Zhang, L.F., 2019. ACS Nano 13 (3), 3714–3722.
Gutierrez-Sanz, O., Andoy, N.M., Filipiak, M.S., Haustein, N., Tarasov, A., 2017. ACS Sens. 2 (9), 1278–1286.

Hao, Z., Zhu, Y.B., Wang, X.J., Rotti, P.G., DiMarco, C., Tyler, S.R., Zhao, X.Z., Engelhardt, J.F., Hone, J., Lin, Q., 2017. Acs Appl. Mater. Interfaces 9 (33), 27504–27511.
Hideshima, S., Sato, R., Inoue, S., Kuroiwa, S., Osaka, T., 2012. Sens. Actuators B Chem. 161 (1), 146–150.
Hostetler, M.J., Templeton, A.C., Murray, R.W., 1999. Langmuir 15 (11), 3782–3789.
Hsiao, C.Y., Lin, C.H., Hung, C.H., Su, C.J., Lo, Y.R., Lee, C.C., Lin, H.C., Ko, F.H., Huang, T.Y., Yang, Y.S., 2009. Biosens. Bioelectron. 24 (5), 1223–1229.
Huang, W.G., Diallo, A.K., Dailey, J.L., Besar, K., Katz, H.E., 2015. J. Mater. Chem. C 3 (25), 6445–6470.
Hwang, H.J., Ryu, M.Y., Park, C.Y., Ahn, J., Park, H.G., Choi, C., Ha, S.D., Park, T.J., Park, J.P., 2017. Biosens. Bioelectron. 87, 164–170.
Jeun, M., Lee, H.J., Park, S., Do, E.J., Choi, J., Sung, Y.N., Hong, S.M., Kim, S.Y., Kim, D. H., Kang, J.Y., Son, H.N., Joo, J., Song, E.M., Hwang, S.W., Park, S.H., Yang, D.H., Ye, B.D., Byeon, J.S., Choe, J., Yang, S.K., Moinova, H., Markowitz, S.D., Lee, K.H., Myung, S.J., 2019. Adv. Sci. 6 (11), 1802115.
Jeun, M., Park, S., Kim, Y., Choi, J., Song, S.H., Jeong, I.G., Kim, C.S., Lee, K.H., 2017. Adv. Health Mater. 6 (17), 1700449.
Kaisti, M., 2017. Biosens. Bioelectron. 98, 437–448.
Latour, R.A., edition, 2nd, Wnek, G.W., Bowlin, G.L. (Eds.), 2008. Encyclopedia of Biomaterials and Biomedical Engineering, vol. 1. Informa Healtcare, pp. 270–284.
Maehashi, K., Katsura, T., Kerman, K., Takamura, Y., Matsumoto, K., Tamiya, E., 2007. Anal. Chem. 79 (2), 782–787.
Nakatsuka, N., Yang, K.A., Abendroth, J.M., Cheung, K.M., Xu, X.B., Yang, H.Y., Zhao, C. Z., Zhu, B.W., Rim, Y.S., Yang, Y., Weiss, P.S., Stojanovic, M.N., Andrews, A.M., 2018. Science 362 (6412), 319–324.
Park, S., Choi, J., Jeun, M., Kim, Y., Yuk, S.S., Kim, S.K., Song, C.S., Lee, S., Lee, K.H., 2017. Adv. Healthc. Mater. 6 (13), 1700371.
Presnova, G., Presnov, D., Krupenin, V., Grigorenko, V., Trifonov, A., Andreeva, I., Ignatenko, O., Egorov, A., Rubtsova, M., 2017. Biosens. Bioelectron. 88, 283–289.
Rajesh Sharma, V., Puri, N.K., Mulchandani, A., Kotnala, R.K., 2016. Appl. Phys. Lett. 109 (24), 243504.
Regonda, S., Tian, R.H., Gao, J.M., Greene, S., Ding, J.H., Hu, W., 2013. Biosens. Bioelectron. 45, 245–251.
Reverberi, R., Reverberi, L., 2007. Blood Transfus. 5 (4), 227–240.
Ruggeri, F., Zhang, F., Lind, T., Bruce, E.D., Lau, B.L.T., Cardenas, M., 2013. Soft Matter 9 (16), 4219–4226.
Saha, K., Agasti, S.S., Kim, C., Li, X.N., Rotello, V.M., 2012. Chem. Rev. 112 (5), 2739–2779.
Seong, T.W., Seo, J., Lee, K.H., 2018. Sens. Actuators B Chem. 267, 237–244.
Sinensky, A.K., Belcher, A.M., 2007. Nat. Nanotechnol. 2 (10), 653–659.
Soler, M., Estevez, M.C., Alvarez, M., Otte, M.A., Sepulveda, B., Lechuga, L.M., 2014. Sensors 14 (2), 2239–2258.
Sun, J.B., Liu, Y.X., 2018. Micromachines 9 (4), 142.
Syu, Y.C., Hsu, W.E., Lin, C.T., 2018. ECS J. Solid State Sci. 7 (7), Q3196–Q3207.
Villamizar, R.A., Maroto, A., Rius, F.X., Inza, I., Figueras, M.J., 2008. Biosens. Bioelectron. 24 (2), 279–283.